DOI: 10.21062/mft.2024.002 http://www.journalmt.com

Application of 35NCD 16 Steel under Cyclic Loading by an Elastoplastic Model

Brahim Chebbab (0000-0002-6678-1394)[1], Mourad Djeziri (0000-0001-5080-9615)[2,3]
[1]Research Unit: Materials. Processes and Environment (UR/MPE). Faculty of technology. University M'hamed Bougara 35000 Boumerdes. Algeria. E-mail: b.chebbab@univ-boumerdes.dz
[2]Center for scientific and technical research in Physico-chemical analysis (CRAPC) BP 384 Bouismail. Tipaza. Algeria. E-mail: m.djeziri@univ-boumerdes.dz
[3]Research Laboratory in Food Technology. Faculty of technology. University M'hamed Bougara of Boumerdes 35000. Algeria. E-mail: m.djeziri@univ-boumerdes.dz

The purpose of this paper is to study an application of the 35NCD 16 steel by a model generalizing the isotropic and kinematic strain hardening laws. The model in question is represented by a field of strain hardening moduli corresponding to the introduction of the configuration of the flow surfaces. Each flow surface is characterized by its constant elastoplastic modulus, its normal unit vector, its radius and its center coordinates. For cases of uniaxial or multiaxial (complex) loading, in particular for cases of cyclic loading or unloading, the instantaneous configuration can be determined by the position and dimensions of the flow surfaces, determining the strain increment for each strain increment.

Keywords: Cyclic plasticity, Three-dimensional elastoplasticity, Incremental elastoplasticity, Plastic flow surface

1 Introduction

The realization of structures in steel construction requires improvements in their use. In this case it's mechanical C in the plastic field, this in order to increase its life. Several researches have been initiated in order to obtain more appropriate models to predict the physical phenomena description that intervene in the solid materials solicited to multiaxial cyclic phenomenological loads [1]. In the field of cyclic solicitations in steels there is an important research as much, at the level of the laws of behavior as well as the experimental determination of the mechanical characteristics and appropriate parameters [2, 3, 4, 5]. Many works have been carried out in this field related to the calculation models of plasticity, such as: Incremental deformations and elastoplastic modulus by introducing isotropic and kinematic strain hardening [6, 7].

Plasticity models are numerous and varied. In the context of our work, we are interested in multisurface plasticity models, which consist of a set of surfaces, the last of which is called the threshold surface. The two-surface models presented by Dafalias & Popov [8], Krieg [9] or Yoshida & Uemori [10] are excluded. Compared to classical plasticity models, multisurface models show very good results in multiaxial under proportional loading. However, they have weaknesses under non-proportional loading, as pointed out by Montans & Caminero [11].

The Mróz model has been extensively studied from a mathematical point of view in the papers by Brokate et al.[12] and Brokate et al.[13]. Nevertheless, some limitations of this model were noted by Jiang & Sehitoglu [14], who observed its inability to describe ratchet effects correctly. They also noted that the response of this model depends on the number of threshold surfaces, and that the translation of each of these surfaces is affected by their number. Jiang & Sehitoglu [14] also concluded that, although Mróz's model seeks to avoid the intersection of threshold surfaces, this can occur in the case of large stress increments. To address this problem, Garud [15] proposed a modification to the Mróz model that adds a condition to make the translation of the threshold surfaces dependent on the stress increment. This modification prevents the threshold surfaces from intersecting even at large stress increments.

A reciprocal theoretical research in plasticity was done simultaneously by Iwan [16] and Mroz [17]. They showed how the flow could be represented by a nesting flow in the stress space. The notion in combination with isotropic and kinematic strain hardening laws can lead to a material representation of considerable power and flexibility. As for Mroz [17], he proposed a model generalizing the isotropic and kinematic strain hardening rules by introducing the notion of "strain hardening modulus, for any loading. The instantaneous configuration is calculated as a function of the translation, expansion or contraction of all flow surfaces. The material behavior can be determined by complex loading trajectories, especially for cases of cyclic loading [17].

Seyed and Yannis [18] applied a two-surface constitutive plasticity model as an effective tool to simulate monotonic and cyclic material behavior.

The two surfaces evolve isotropically and kinematically in the stress space. Compared to the infinitesimal plasticity of Von Mises, the multiaxial cyclic loading gave the idea proposed by the model of Mroz. As for Meijuan et al. [19] compared the Besseling type model to large deformations using hyperelasticity and classical Kröner-Lee multiplicative decompositions. Nobutada et al. [20] worked on the preloading resulting from the maximum plastic deformation. To evaluate the range of cyclic plastic deformation in the preloading presence, A set of evolution equations have been proposed. These extensions are verified by performing uniaxial cyclic experiments of 316 stainless steel at 600°C. The experiments are accurately simulated using a model. Changes Jisheng et al. [21] have qualitatively described the response to dual strain path changes in low carbon steels. Abdelmalek et al. [22] have demonstrated the buckling instability of a steel beam subjected to multiaxial loads using an approximate Ritz method under an ABAQUS code. Ritz method under an ABAQUS calculation code.Where the numerical implementation of a model that predicts directional hardening only for strain path changes involving unloading and reloading, was presented by Wang et al. [23].

The purpose of this study is to apply by modeling the flow surfaces characteristics for any loading or unloading point of an element of the structure to be considered.

2 Model description

Mroz [9] considers that there are several interlocking flow surfaces. He assigns a plastic modulus to these surfaces and thus models the cyclic behavior of metals. Knowing that the surfaces are concentric circles, he explains how these surfaces evolve. The first flow surface is represented by the elastic domain where the loading point is located in the stress space.

By activating the loading point on the first circle surface C0. The latter moves with it in the same way as in kinematic strain hardening, which determines the plastic modulus value H0. The direction of translation of the circle C0 is dictated by a normal vector ni to the surface.

On reaching the stress point C1. It is activated and the plastic modulus is then H1. The direction of translation is given by a new loading point located on the circle C1 and so on.

3 Assumptions

Assumptions must be made for an easier development of the constitutive relations and to limit the validity domain of the proposed model. Classically the assumptions made by a large number of authors are initial material homogeneities, the total deformation is the sum of a reversible elastic component and an irreversible plastic component, deformation of theoretical origin not taken into account and existence of an initial elastic domain. It is a question of defining in the constraints. a convex domain of elasticity inside which the irreversible plastic deformations are almost non-existent. The mathematical expression of this domain is given by the function which depends. For isotropic materials on the three invariants of the stress tensor, this domain translates, rotates grows and deforms during the deformation of the material. However, we will retain only its translation and expansion responsible respectively for kinematic and isotropic strain hardening, the first is characterized by a tensor quantity X and the second by a scalar R. These quantities are introduced as internal variables. Normality of the plastic strain rate and plastic incompressibility.

4 Modeling

In a Cartesian system of orthogonal coordinates (1.2.3).

We have:

$$\sigma_{33}=\sigma_{23}=\sigma_{13}=\sigma_{22}=0 \tag{1}$$

And the non-zero components in the (1.2) plane are: $(\sigma_{11},\sigma_{12})$.

$$\sigma_{ij}=\begin{bmatrix}\sigma_{11} & \sigma_{12} & 0\\ \sigma_{12} & 0 & 0\\ 0 & 0 & 0\end{bmatrix}\text{[Mpa]} \tag{2}$$

$$X_{ij}=\begin{bmatrix}X_{11} & X_{12} & 0\\ X_{12} & 0 & 0\\ 0 & 0 & 0\end{bmatrix}\text{ [mm]} \tag{3}$$

$$\sigma_{ij}^{'}=\sigma_{ij}-\frac{1}{3}\delta_{ij}(\sigma_{kk})\text{ [Mpa]} \tag{4}$$

$$X_{ij}^{'}=X_{ij}-\frac{1}{3}\delta_{ij}(\sigma_{kk})\text{ [mm]} \tag{5}$$

Where:

σ_{ij} …Stress tensor [Mpa];

X_{ij} …Center of the flow surfaces in the stress space [mm];

$\sigma_{ij}^{'}$ …Deviatorial stress tensor [Mpa];

$X_{ij}^{'}$ …Center of flow surfaces in deviatoric stress space [mm];

δ_{ij} …Kronecker symbol;

σ_{kk} …Mean stress tensor [Mpa].

$$\sigma_{ij}^{'}=\begin{bmatrix}\frac{2}{3}\sigma_{11} & \sigma_{12} & 0\\ \sigma_{12} & -\frac{1}{3}\sigma_{11} & 0\\ 0 & 0 & -\frac{1}{3}\sigma_{11}\end{bmatrix}\text{[Mpa]} \tag{6}$$

$$X_{ij}^{'}=\begin{bmatrix}\frac{2}{3}X_{11} & X_{12} & 0\\ X_{12} & -\frac{1}{3}X_{11} & 0\\ 0 & 0 & -\frac{1}{3}X_{11}\end{bmatrix}\text{[mm]} \tag{7}$$

Where:

$$\sigma_{ij}^{'}-X_{ij}^{'}=\begin{bmatrix}\frac{2}{3}(\sigma_{11}-X_{11}) & \sigma_{12}-X_{12} & 0\\ \sigma_{12}-X_{12} & -\frac{1}{3}(\sigma_{11}-X_{11}) & 0\\ 0 & 0 & -\frac{1}{3}(\sigma_{11}-X_{11})\end{bmatrix}\text{[mm]} \tag{8}$$

$$\left\{\left[\frac{2}{3}(\sigma_{11}-X_{11})\right]^2+2\left[-\frac{1}{3}\left(\sigma_{11}-X_{11}\right)\right]^2+2\left(\sigma_{12}-X_{12}\right)^2\right\}=\frac{2}{3}R^2\text{ [mm]} \tag{9}$$

$$\frac{2}{3}\left(\sigma_{11}-X_{11}\right)^2+2\left(\sigma_{12}-X_{12}\right)^2=\frac{2}{3}R^2\text{ [mm]} \tag{10}$$

According to the Von Mises criterion [3]. The flow function in the plane is expressed by the following relation:

$$\left(\sigma_{11}-X_{11}\right)^2+3\left(\sigma_{12}-X_{12}\right)^2=R^2\text{ [mm]} \tag{11}$$

From the above equation, we obtain flow surfaces in the form of ellipses.

Assuming that the flow law is associated and that the normal vectors outside the flow surfaces are identical, this law is expressed by the following relation:

$$d\varepsilon_{ij}^{p}=\frac{d\sigma_{ij}}{H_p}\text{ [mm]} \tag{12}$$

With:

$$n_{ij}=\frac{\partial f}{\|\partial f\|}=\frac{\sigma_{ij}-X_{ij}}{\|\sigma_{ij}-X_{ij}\|} \tag{13}$$

Where:

f …The load function.

$$d\vec{\sigma}=d\vec{\sigma}.\vec{n}_{ij}\text{ [Mpa]} \tag{14}$$

$d\vec{\sigma}$ is the stress increment projection $d\vec{\sigma}$ on the unit vector $\vec{n}_{ij}$ normal to the flow surface and H_p the tangent elastoplastic modulus.

$$H_p=\frac{d\sigma_{ij}}{d\varepsilon_{ij}^{p}}\text{ [Mpa]} \tag{15}$$

Elastoplastic moduli are also calculated as a function of equivalent stress K_y and M_y material-dependent parameters.

$$H_p=k(p)=\frac{K_y}{M_y}p^{\frac{1-M_y}{M_y}}=\frac{K_y}{M_y}\left(\frac{R-\sigma_y}{K_y}\right)^{1-M_y}\text{ [Mpa]} \tag{16}$$

Where:

$$R = \sigma_y + K_y \left(H_p \frac{M_y}{K_y} \right)^{\frac{1}{1-M_y}} \text{[mm]} \tag{17}$$

R …Radius of the flow surface.

The incremental plastic deformations are calculated for each flow surface:

$$d\varepsilon_{ij}^{p} = \frac{3}{2} \frac{M_y}{K_y} \left(\frac{\sigma_{eq} - \sigma_y}{K_y} \right)^{M_y - 1} \frac{\langle d\sigma_{eq} \rangle}{\sigma_{eq}} \sigma_{ij}^{'} \text{[mm]} \tag{18}$$

Keeping unchanged and proceeding to a change of axis σ_{12} . in $\sqrt{3}\,\sigma_{12}$. We obtain circles which are concentric to the origin O.

5 Results

The model presents a large number of flows surfaces each flow surface is represented by an elastoplastic modulus H, the flow surfaces are contained in the boundary surface of size R_{max}, Figures 1, 2 and 3 illustrate perfectly two types of flow surfaces:

- Non-active flow surfaces are surfaces that have never been reached or moved by the "current" stress points. The kinematic strain hardening can be said to depend on the degradation parameters. But the direction of deformation is not especially in the path of the stress point.
- Active flow surfaces are surfaces that have reached or moved by the "current" stress points. It can be said that the kinematic strain hardening depends not only on the degradation parameters, but also on the stress paths; and therefore, the translation of the flow surface is indicated to use by the kinematic strain hardening rule. In their work, Iwan and Mroz confirmed the extension in the case of multiaxial loading [16, 17].

5.1 Case 1: Bi-axial cyclic loading along the x and y axes

When the biaxial stress (normal and tangential stress) lies within the smallest "threshold" surface, each described by the Von Mises criterion (surface f0 in Fig. 1), the model's behavior is elastic. Each time the biaxial "threshold" stress is loaded by an increment of loading or unloading stress, it becomes active and reaches a new "threshold" surface. The plastic flow of the structure results in a new flow surface configuration, which is described by the coordinates of its center, the size of the flow surface, the components of its normal vector, which depends on the direction of flow, and by the value of its elastoplastic modulus. This new flow surface configuration is thus called a new reference group. During flow, the active surface always respects the flow surface condition f = 0.

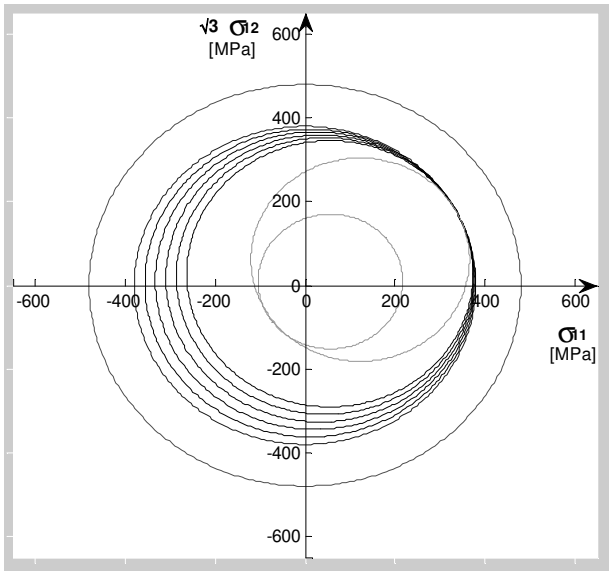

Fig. 1 *Operation of the Mroz model Successive cyclic loading case: tensile stress then shear*

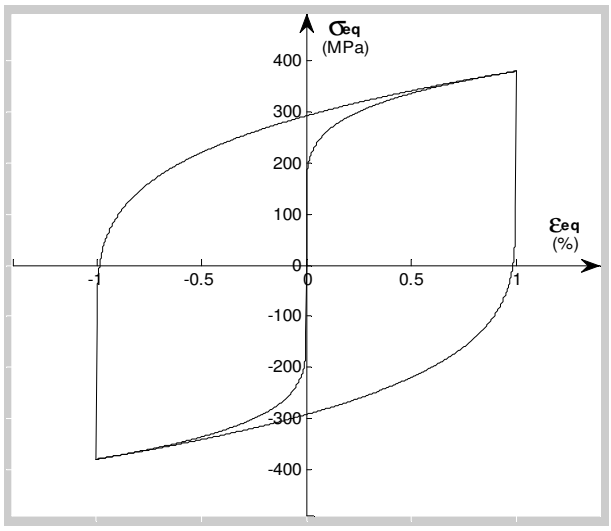

Fig. 2 *Multiaxial cyclic loading (stress and tangential)*

Figure 2 shows the stress-strain curve. It describes cyclic and biaxial loading, represented by segments of constant tangent modulus.

It can be seen that the elastoplastic H modulus of the flow surfaces is inversely proportional to loading. They depend solely on the degradation parameter, while converging towards a zero value (the value considered as the elastoplastic modulus at rupture Hu).

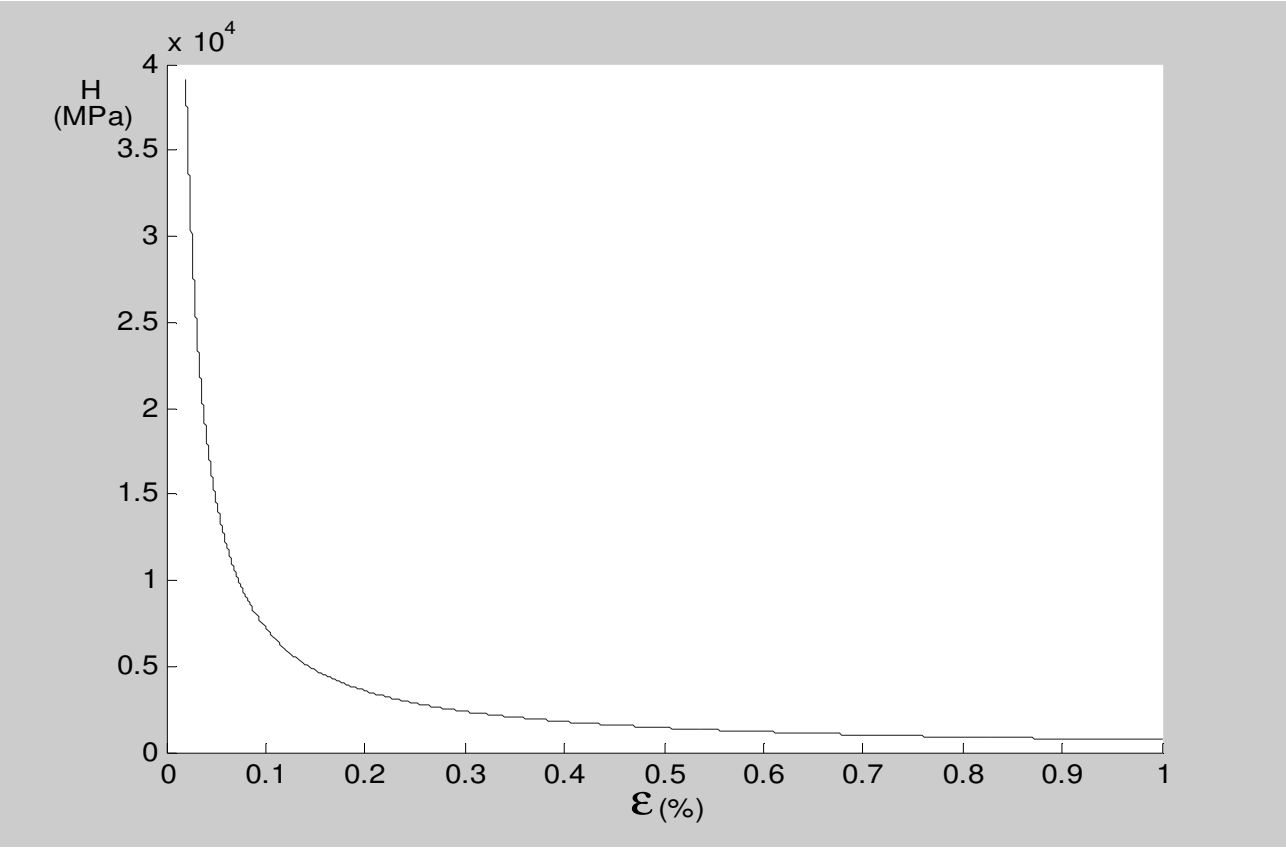

Fig. 3 *Elastoplastic moduli as a function of equivalent plastic strain*

Tab. 1 *Characteristics of the active surfaces of the 1st reference group*

R	σ_{11}	σ_{12}	x_0	y_0
(mm)	(Mpa)	(Mpa)	(mm)	(mm)
318.3349	190.1	141.2048	55.25619	27.62809
330.6376	199.4	145.8548	44.25228	22.12614
342.9404	208.7	150.5048	33.24837	16.62418
355.2431	218	155.1548	22.24446	11.12223
367.5459	227.3	159.8048	11.24055	5.620276
380.1132	236.8	164.5548	0	0

Tab. 2 *Characteristics of the 1st reference group*

R	σ_{11}	σ_{12}	x_0	y_0	n_x	n_y	H
(mm)	(Mpa)	(Mpa)	(mm)	(mm)	-	-	(Mpa)
380.1132	236.8	164.5548	0	0	0.622972	0.749822	711.7612

During incremental loading of the biaxial stress, the results obtained in tables 1 and 2 of the first reference group show that the flow surface has increased in size and that the coordinates of the center of the active flow surface are increasingly close to the "threshold" flow surface. The components of the normal vector maintain flow normality, while determining the value of the elastoplastic modulus at the position of the "threshold" surface.

Tab. 3 *Characteristics of the active surfaces of the 2nd reference group*

R	σ_{11}	σ_{12}	x_0	y_0
(mm)	(Mpa)	(Mpa)	(mm)	(mm)
242.9619	-63.2	-135.445	122.6718	61.33592
161.086	-15.2	-92.5881	56.5	9.185742

Tab. 4 *Characteristics of the 2nd reference group*

R	σ_{11}	σ_{12}	x_0	y_0	n_x	n_y	H
(mm)	(Mpa)	(Mpa)	(mm)	(mm)			(Mpa)
242.9619	-63.2	-135.445	122.6718	61.33592	0.355863	-0.93454	5755.13

The results obtained in tables 3 and 4 of the second reference group, during biaxial stress unloading, show that the flow surface has undergone a significant reduction in size, and the coordinates of the center of the active flow surface are getting closer and closer to the threshold flow surface. The components of the associated vector always retain flow normality.

5.2 Case 2: Case of uniaxial cyclic loading along the x axis

When the uniaxial stress (tensile or compressive normal stress) lies within the smallest threshold surface described by the Von Mises criterion (surface f0 in Fig. 4), the model's behavior is elastic. During loading or unloading of the uniaxial normal stress by an increment, the flow surface becomes active and translates to become tangent with a new surface. As a result, plastic flow and structure give rise to a new surface configuration, with new center coordinates and a new flow surface size. The components of the direction-dependent vector retain the flow normal and the value of its elastoplastic modulus. The result is a new reference group.

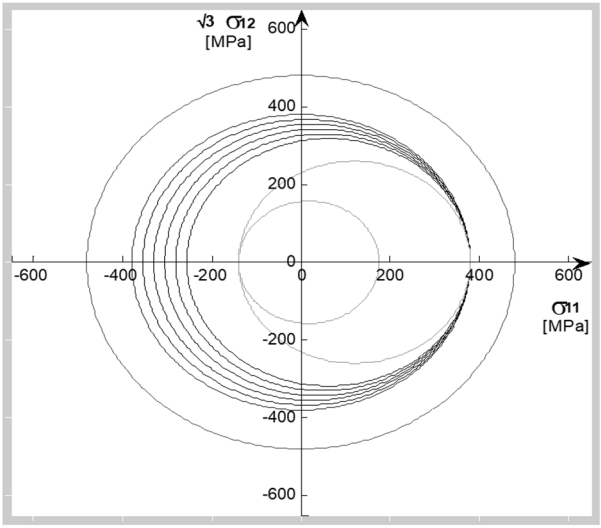

Fig. 4 *Operation of the Mroz model cyclic uniaxial loading case normal tension-compression stress*

Tab. 5 *Characteristics of the active surfaces of the 1st reference group*

R	σ_{11}	σ_{12}	x_0	y_0
(mm)	(Mpa)	(Mpa)	(mm)	(mm)
318.3	318.3	0	61.7	0
330.6	330.6	0	49.4	0
342.9	342.9	0	37.1	0
355.2	355.2	0	24.8	0
367.5	367.5	0	12.5	0
380	380	0	0	0

Tab. 6 *Characteristics of the 1st reference group*

R	σ_{11}	σ_{12}	x_0	y_0	n_x	n_y	H
(mm)	(Mpa)	(Mpa)	(mm)	(mm)			(Mpa)
380	380	0	0	0	1	0	712.919573

During incremental loading of the uniaxial stress (tensile or compressive stress), the results obtained in tables 6 and 7 of the first reference group showed that the flow surface increased in size and the coordinates of the center of the active flow surface increasingly approached the threshold flow surface. The components of the normal vector maintain the normality of the flow, while determining the value of the elastoplastic modulus at the position of the "threshold" surface.

Tab. 7 *Characteristics of the active surfaces of the 2nd reference group*

R	σ_{11}	σ_{12}	x_0	y_0
(mm)	(Mpa)	(Mpa)	(mm)	(mm)
260	-260	0	120	0
157.6	-157.6	0	17.6	0

Tab. 8 *Characteristics of the 2nd reference group*

R	σ_{11}	σ_{12}	x_0	y_0	n_x	n_y	H
(mm)	(Mpa)	(Mpa)	(mm)	(mm)			(Mpa)
260	-260	0	120	0	-1	0	9247.43525

The results obtained in tables 7 and 8 of the second reference group show that, under uniaxial stress unloading (tensile or compressive stress), the flow surface undergoes a significant reduction in size, and the coordinates of the center of the active flow surface move closer and closer to the "threshold" surface. The components of the associated vector always maintain flow normality.

5.3 Case 3: Case of uni axial cyclic loading along the y-axis

When the uniaxial stress (tangential stress) lies within the smallest threshold surface described by the Von Mises criterion (surface f0 in Fig.5), the model's behavior is elastic. Each time we load or unload the uniaxial normal stress by an increment, it becomes active and translates, where it becomes tangent with a new "threshold" surface. Plastic flow and structure give rise to a new threshold surface configuration, new center coordinates and a new flow surface size. The components of the associated direction-dependent vector maintain the flow's normality, with a new value for its elastoplastic modulus. The result is a new reference group.

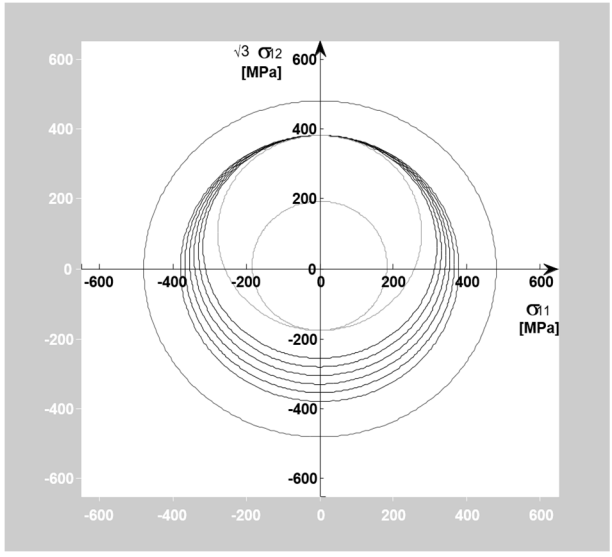

Fig. 5 *Operation of the Mroz model case of uniaxial cyclic stress-shear loading*

Tab. 9 *Characteristics of the active surfaces of the 1st reference group*

R	σ_{11}	σ_{12}	x_0	y_0
(mm)	(Mpa)	(Mpa)	(mm)	(mm)
318.33	0	183.787586	0	61.8342138
330.63	0	190.887586	0	49.5366531
342.92	0	197.987586	0	37.2390924
355.22	0	205.087586	0	24.9415316
367.52	0	212.187586	0	12.6439709
380.16	0	219.487586	0	0

Tab. 10 *Characteristics of the 1st reference group*

R	σ_{11}	σ_{12}	x_0	y_0	n_x	n_y	H
(mm)	(Mpa)	(Mpa)	(mm)	(mm)	-	-	(Mpa)
380.16365	0	219.487586	0	0	0	1	711.245269

From the results obtained in tables 9 and 10 of the first reference group, we can see that the uniaxial stress (tensile or compressive stress) and the flow surface have increased in value and size respectively.

The coordinates of the center of the active flow surface are increasingly close to the threshold surface. The components of the vector maintain flow normality, while determining the value of the elastoplastic modulus at the position of the "threshold" surface.

Tab. 11 *Characteristics of the active surfaces of the 2nd reference group*

R	σ_{11}	σ_{12}	x_0	y_0
(mm)	(Mpa)	(Mpa)	(mm)	(mm)
278.015657	0	-160.512414	0	102.147994
183.990041	0	-106.2267	0	8.12237834

Tab. 12 *Characteristics of the 2nd reference group*

R	σ_{11}	σ_{12}	x_0	y_0	n_x	n_y	H
(mm)	(Mpa)	(Mpa)	(mm)	(mm)			(Mpa)
278.015657	0	-160.512414	0	102.147994	0	-1	16381.316

The results obtained in tables 11 and 12 above for the second reference group, during uniaxial stress unloading (tangential stress) show that the flow surface has undergone a significant reduction in size, and the coordinates of the center of the active flow surface converge towards the center of the "threshold" flow surface. The components of the associated vector still maintain flow normality.

6 Discussions

According to the results obtained in all the figures shown, we deduce that during loading, the elastoplastic modulus increases with small cumulative variations, unlike during unloading. We observe that the elastoplastic modulus increases significantly. This explains the phenomenon of isotropic strain-hardening, as the size of the flow surface takes on a new dimension, providing a large elastic domain. During loading or unloading, the diagrams show translations of the flow surfaces, from which we deduce that the center of the flow surface takes on new coordinates, which shows us the kinematic strain-hardening phenomenon [6, 7].

However, we would point out that the steels used in this work do not show ratchet effects in cyclic loading, as pointed out by Brokate et al. [12], and that heat treatment contributes to an adequate increase in residual service life, as reported by Petr Beneš, et al. [24]. Note that, for the case of loading or unloading according to the normal or tangential contraction of the structural element, the coordinates of the center of the active flow surface translate uniaxially as a function of the loaded or unloaded contraction. However, in the case of biaxial loading or unloading, the coordinates of the center of the active flow surface translate in the quadrant axes. In view of the results obtained, we observe that the yield stress at unloading is significant compared to loading. Plastic flow always obeys the rule of the associated flow law.

Figures 1, 2 and 3 also illustrate the variation of elastoplastic modulus as a function of cumulative plastic deformation. These variations are represented by hyperbolic curves. The results obtained give us the values of the elastoplastic modulus. We can see that the elastoplastic modulus H of the flow surfaces are inversely proportional to the loads and depend only on the degradation parameter while converging towards a null value (Value considered as elastoplastic modulus at break H_u). Since the flow surfaces are defined by their elastoplastic modulus (H), the areas outside two flow surfaces are therefore limited by Elastoplastic modulus (H_o), The boundary between the active and the non-active zone (H_p)and Ultimate elastoplastic modulus (V).

The work hardening rule of the original flow surface describes the loading of the material behavior. When plastic deformations are induced in the latter, we notice that there is a change of position (X_o and Y_o) and of size R in the flow surface.

7 Conclusion

In this work we have presented a program that determines the groups of flow surfaces of a structural element subjected to cyclic and multiaxial loading in the plastic domain by an elastoplastic model of Mroz. To achieve these possibilities, we proceeded to the modeling by incrementing the nonlinear part "by piece" of the curve "stress-strain" in a three-dimensional case. For this purpose, we have considered the following points: Choice of a plasticity flow criterion according to the type of material to be used and its ease of use, choice of the plastic flow law, the model combines isotropic and kinematic properties to represent the idea of a plastic modulus field defined in the stress space by the relative configuration of the flow surfaces and definition of the groups whose material behavior is known by its mechanical characteristics following the

imposed loading.

From the results obtained, we can conclude that we can update at each instant, for each flow surface, its size, its components of its normal unit vector and its elastoplastic modulus.

On the other hand, the program also deals with the identification of the flow surface for any loading or unloading point. For this, we have established an algorithm that allows determining the characteristics of the flow surface to which the loading point belongs.

The response of this model is dependent on the number of "threshold" surfaces; in particular, the translation of each surface is affected by its number. Compared with more conventional plasticity models, multi-surface models show very good multiaxial results under proportional or non-proportional loading. This model was applied to the plasticity of soils, but for our purposes, we have integrated it into the plasticity of solid materials, in this case steels, as described in this work.

The interest of this model lies in its very low number of parameters compared to other models of plasticity with work hardening.

Given the complexity of nonlinear plasticity, we wish to continue this work with the Mroz model for multiaxial and cyclic loading and to see the possibility of integrating other factors that influence the deformation of the flow surface.

Acknowledgement

Our warmest thanks to the members of the research unit: Materials, Processes and Environment (UR/MP), Faculty of technology, University M'hamed Bougara, Boumerdes, Algeria for their technical support.

References

[1] LUONG, M. P. (1980). Phénomènes cycliques dans les sols pulvérulents. In : *Revue Française de géotechnique*, Vol, 10. No. 2, pp. 39 – 53. ISSN 0181– 0529

[2] KLINSKI, M. (1988). A cyclic plasticity model based on fuzzy set theory. In: *Journal of engineering Mechanics ASCE*, Vol. 114. No 4, pp. 563 – 582. ISSN 0733 – 9399

[3] CHABOCHE, J. L. (1989). Constitution equation for cyclic plasticity and cyclic viscoplasticity. In: *International Journal of Plasticity*, Vol. 51. No 3, pp. 247– 302. ISSN 1879 –2154

[4] ACHIALLEAS, G. P., GEORGE, D. B. (2002). Plasticity model for under sand small and large cyclic strain: multiaxial formulation. In: *Soil Dynamics and Earthquake engineering*, Vol. 22, pp. 191 – 204. ISSN 1879-341X

[5] VERONIQUE A. (2001). Plasticité cyclique d'un acier inoxydable austéno-ferritique sous chargement biaxial non-proportionnel. Matériaux. *Université des Sciences et Technologie de Lille - Lille I; Ecole Centrale de Lille. Français*. NNT. Tel-00005814v2.

[6] THOMAS, B. S., JEONG, W. Y. (2018). Kinematic hardening model considering directional hardening response. In: *International Journal of Plasticity*, Vol. 110, pp. 145 – 165. ISSN 1879 –2154

[7] KNUT, M., MAGNUS, E., JOHAN, A. (2018). Modeling of kinematic hardening at large biaxial deformations in pearlitic rail steel. In*: International Journal of Plasticity*, Vol. 130-131, pp. 122 –132. ISSN 1879 –2154

[8] DAFALIAS, Y. F., POPOV, E. P. (1975). A model of non –linearly hardening materials for complex loading. In: *Acta Mechanica*, Vol. 21, pp. 173 –192. ISSN 1619 – 6937

[9] KRIEG, R. D. (1975). A practical two surface plasticity theory. In*: Journal of Applied Mechanics*, Vol. 42. No. 3, pp. 641– 646. ISSN 0021– 8936

[10] YOSHIDA, F., UEMORI, T. (2022). A model of large-strain cyclic plasticity describing the Bauschinger effect and work hardening stagnation. In: *International Journal of Plasticity*, Vol. 18, pp. 661– 686. ISSN 1879 –2154

[11] MONTANS, F. J., CAMINERO, M. A. (2007). On the consistency of nested surfaces, models and their kinematic hardening rules. In: *International Journal of Solids and Structures*, Vol. 44, pp. 5027–5042. ISSN 1879– 2146

[12] BROKATE, M., DRESSLER, K, KREJCI, P. (1996). On the Mróz model. In: *European Journal of Applied Mathematics*, Vol. 7. No. 5, pp. 473 – 497. ISSN 1469– 4425

[13] BROKATE, M., KREJCI, P., RACHINSKII, D. (1998). Some analytical properties of the multidimensional continuous Mróz model of plasticity. In: *Control and Cybernetics*, Vol. 27. No. 2, pp. 199–215. ISSN 2720– 4278

[14] JIANG, Y., SEHITOGLU, H. (1996). Comments on the Mróz multiple surface type plasticity models. In: *International Journal of Solids and Structures*, Vol. 33. No. 7, pp. 1053 –1068. ISSN 1879–2146

[15] GARUD, Y. S. (1981). A New Approach to the Evaluation of Fatigue under Multiaxial Loadings. In: *Journal of Engineering Materials and Technology*, Vol. 103. No. 2, pp. 118 –125. ISSN 0094 – 4289

[16] IWAN, W. D. (1967). On a class of models for yieldin behavior of continuo and composite system. In: *Journal of Applied Mechanics*, Vol. 67. Trans ASME. Serie E. No.9, pp. 612–617. ISSN 0021– 8936

[17] MROZ, Z. (1967). On the description of anisotropic work hardening. In: *J Mech.Phys. Solids*,Vol. 15, pp. 163–175. ISSN: 1873 – 4782

[18] SEYED, B. B, YANNIS, F. D. (2022). Modeling Fundamentals and Applications. In: *Elsevier Series on Plasticity of Materials*, pp. 101–138. ISBN 9780128192931

[19] MEIJUAN, Z., et al. (2022). Cyclic Plasticity of Metals Modeling Fundamentals and Applications. In: *Elsevier Series on Plasticity of Materials*, pp. 55–100. ISBN 9780128192931

[20] NOBUTADA, O., et al. (2021). Modeling of cyclic hardening and evaluation of plastic strain range in the presence of pre-loading and ratcheting. In: *International Journal of Plasticity*, Vol. 145, pp. 103–174. ISSN 1879 –2154

[21] JISHENG, Q., BJØRN, H., ODD, S. H. (2018). A combined isotropic. Kinematic and distortional hardening model for aluminum and steels under complex strain-path changes. In: *International Journal of Plasticity*, Vol. 101, pp. 156–169. ISSN 1879 –2154

[22] ABDELMALEK, K., et al. (2021). Mathematical modeling and numerical simulation of the buckling stability behavior of hybrid beam. In: *Manufacturing technology engineering science and research journal*, Vol. 21. No. 6, pp. 793–804**.** ISSN 1213–2489

[23] WANG, J. L., EVKOVITCH, V., SVENDSEN, B. (2006). Modeling and simulation of directional hardening in metals during non-proportional loading. In: *J. Mater. Process. Technol*, Vol. 177, pp. 430–432. ISSN 1873–4774

[24] PETR, B., et al. (2023). Possibilities of Restoring the Plasticity of Operationally Degraded Steel EN ISO 14MoV6-3. In : *Manufacturing technology engineering science and research journal*, Vol. 23. No. 5, ISSN 1213–2489 (online)